Electronic Supplementary Information

The Topology Design Principles that Determine the Spatiotemporal Dynamics of G-protein Cascades.

Mikhail A. Tsyganov[1,2], Walter Kolch[2] and Boris N. Kholodenko[2,3*]

[1]Institute of Theoretical and Experimental Biophysics, Pushchino, Moscow Region, Russia

[2]Systems Biology Ireland, University College Dublin, Belfield, Dublin 4, Ireland,

[3]Thomas Jefferson University, Department of Pathology, Anatomy, and Cell Biology, Philadelphia, PA 19107, USA

Supplementary Figures.

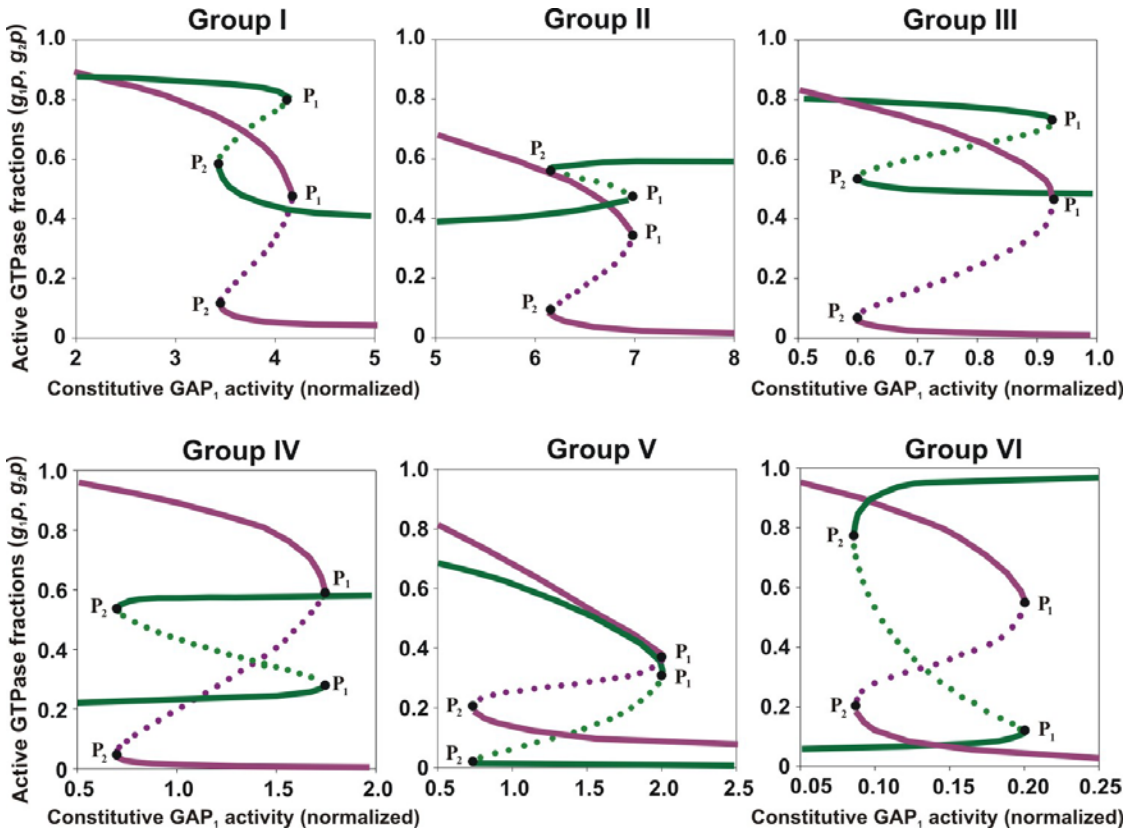

Fig. S1. Bistability and hysteresis in GTPase cascades in groups I - VI: responses to gradual changes in GAP_1 concentrations. Hysteretic behavior of the steady-state responses of active GTPase fractions, g_1p (purple) and g_2p (green), to the changes in the input GAP_1 activity (parameter r_2) are shown. Dotted lines correspond to unstable steady states located at the intermediate branch of the curve between turning points P_1 and P_2 (marked bold). The dependencies of steady-state responses on parameters are identical for all eight designs within a group, if the relationships between kinetic parameters enabling the identity of steady states are satisfied (see Table 1, Methods). For each group I - VI, the hysteresis curves are calculated for topology design 1, whose kinetic parameters are given in Table S1 where parameter r_2 is varied in the ranges shown (s^{-1}). Note that the stationary, active GTPase fractions behave similarly when the input GEF or GAP activity is changed by altering the strength of the autocatalytic loop (given by values of the multiplies α_{11} and α_{12}, Eq.4, Methods) rather than by changing the maximal rate r_1 or r_2.

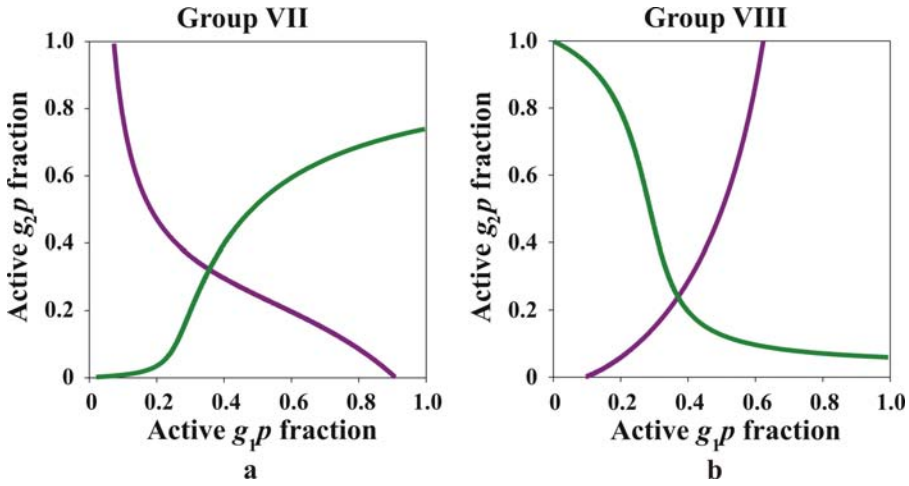

Fig.S2. Typical nullcline shapes for 16 cascade topologies that comprise VII and VIII groups. (**a**). Group VII. The g_1p-nullcline (purple) is a monotone decreasing function of g_1p and the g_2p-nullcline (green) is a monotone increasing function of g_1p, which cannot intersect at more than one point. (**b**). Group VIII. The g_1p-nullcline (purple) is a monotone increasing function of g_1p and the g_2p-nullcline (green) is a monotone decreasing function of g_1p, and, therefore, these two nullclines cannot intersect at more than one point. Kinetic parameters are the following: (**a**) r_1= 1, r_2= 0.13, r_3= 10, r_4= 30 (s^{-1}), m_1= 0.4, m_2=0.09, m_3= 2, m_4= 0.01, a_{11}= 0.6, m_{11}= 0.1, a_{13}= 100, m_{13}= 3, a_{21}= 0.01, m_{21}= 0.1; (**b**) r_1= 1, r_2= 1.5, r_3= 1, r_4= 0.01 (s^{-1}), m_1= 1, m_2=5, m_3= 0.1, m_4= 0.05, a_{11}= 0.01, m_{11}= 0.005, a_{13}= 0.004, m_{13}= 0.002, a_{21}= 100, m_{21}= 2.

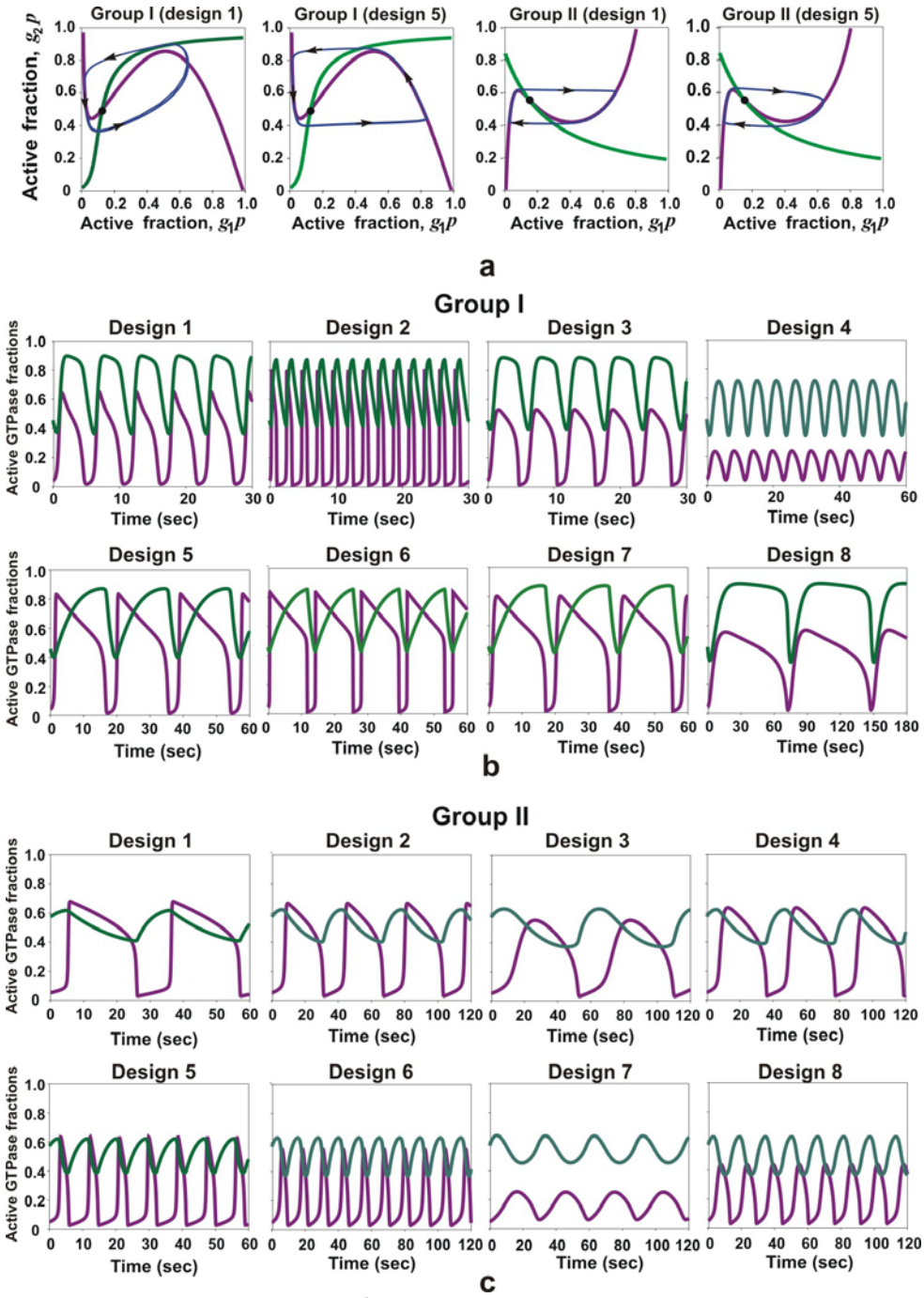

Fig. S3. Oscillatory regimes of 16 cascades comprising groups I and II. (a) The g_1p-nullclines (purple, N-mirror shaped, group I, and N-shaped, group II) and the g_2p-nullclines (green, monotone) intersect at a single point (marked in bold) corresponding to an unstable steady state. The limit cycle trajectories (blue) on the plane (g_1p, g_2p) are shown for kinetic designs 1 and 5. Arrows indicate the direction of motion. (**b**, **c**) Sustained oscillations of active GTPase fractions (g_1p, purple and g_2p, green) are shown for all kinetic designs comprising groups I and II. Kinetic parameters are presented in Table S2 for design 1, and the parameter value relationships for other designs are specified in Table 1 (Methods). For illustrative purposes, for design 4 in group I the constitutive GEF_1 and GAP_1 activities were increased by a factor of 2 compared to the activities presented in Table S2, as follows, r_1= 10, r_2= 8 (s^{-1}).

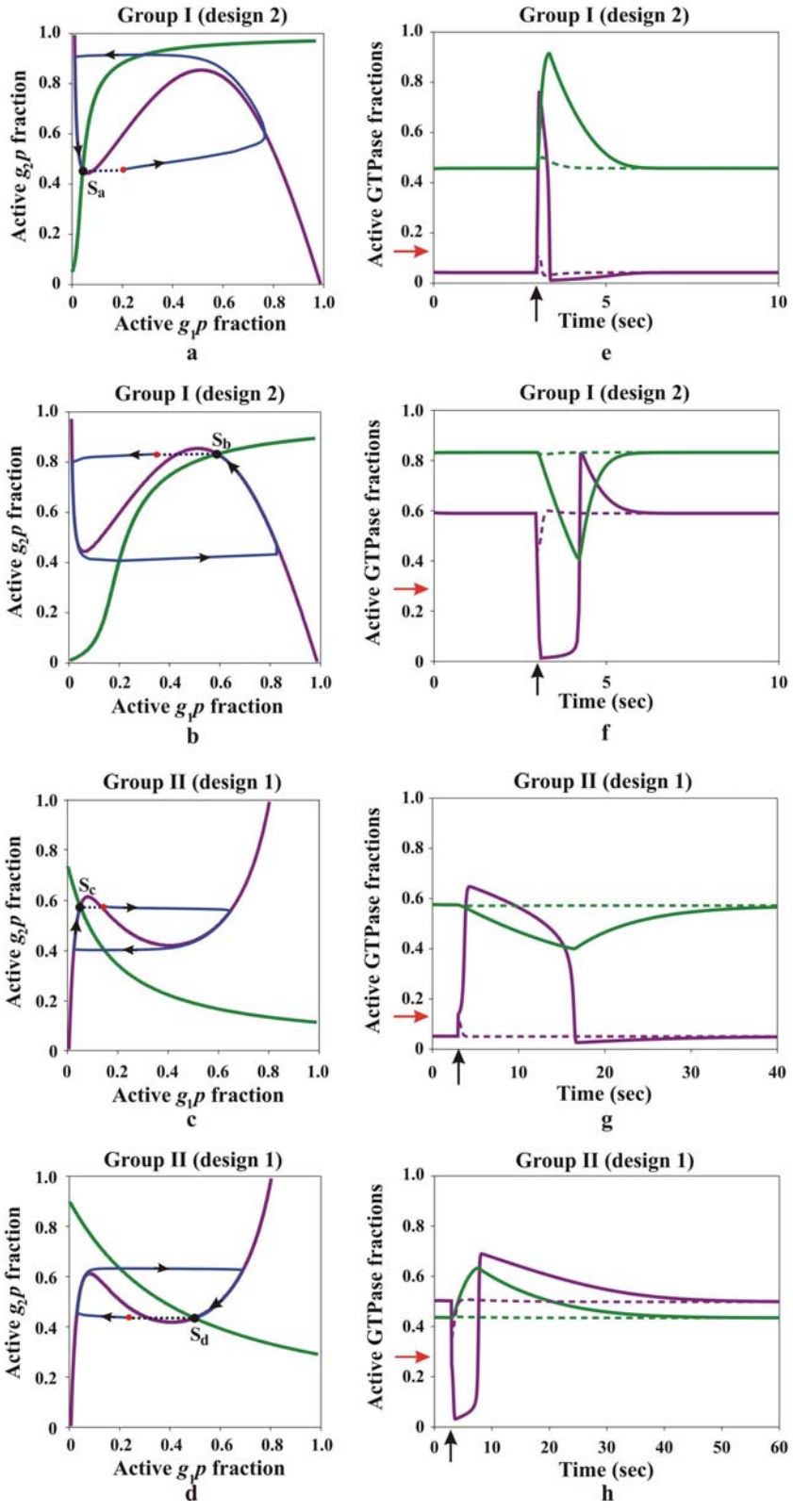

Fig. S4. Excitable behavior of GTPase cascades. Initially, each cascade resides in a stable, but excitable steady state. For group I cascades (**a, b**), the first g_1p-nullcline (purple) is N-mirror shaped, and the second g_2p-nullcline (green) is a monotone increasing function of g_1p. For group II cascades (**c, d**), the first g_1p-nullcline (purple) is N- shaped, and the second g_2p-nullcline (green) is a monotone

decreasing function of g_1p (**a - d**). The two nullclines intersect at a single point, corresponding to a stable steady state (S, bold black dot) positioned at the left arm (**a**, **c**) or the right arm (**b**, **d**) of the g_1p-nullcine. The different steady state positions are brought about by the changes in GEF_2 activity, described by the parameter r_3, whose magnitudes and the corresponding steady-state values of GTPase fractions (g_1p_{ss}, g_2p_{ss}) are given in Table S2. The trajectories (blue) presented on the phase plane (g_1p, g_2p) correspond to over-threshold perturbations (shown by dotted lines which start with steady-state values **S** and end with red dots). Panels (**e - h**) show temporal responses of active GTPase fractions, g_1p (purple) and g_2p (green), to sub-threshold (dashed lines) and over-threshold (solid lines) perturbations. At time t = 3 s (marked by black arrow), the steady-state concentration of the active GTPase at the first level (g_1p) is perturbed. Sub-threshold perturbations cause small responses shown by dashed lines. Over-threshold perturbations cause large overshoot responses where the active GTPase fractions can significantly increase or decrease, generating temporal pulses of GTPase activities (threshold values of g_1p perturbation amplitudes are marked by red arrows). It is instructive to note that while GEF_2 activity (r_3) varies (decreases for group I cascades or increases for group II cascades), the excitable regime, corresponding to the stable steady state positioned at the left arm of the g_1p-nullcline (**a**, **c**) becomes oscillatory, corresponding to the unstable steady state positioned at the middle arm (Fig. S3a). With a further change in r_3, the oscillatory regime becomes again excitable, corresponding to the stable steady state positioned at the left arm of the g_1p-nullcline (**b**, **d**).

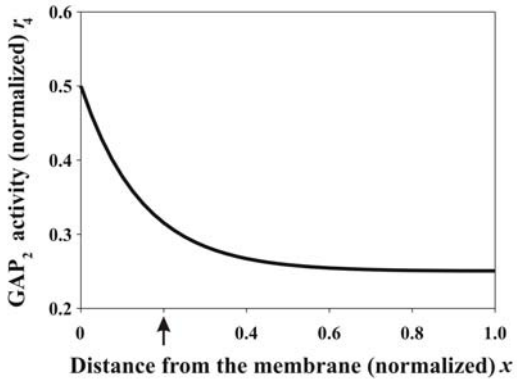

Fig. S5. Spatial gradient of GAP_2 constitutive activity. The activity (r_4) of GAP_2 decreases with the distance (x) from the plasma membrane, as specified by Eq. 10 in Methods. The kinetic parameter values are the following, $r_4(0)=0.5$, $r_4(1)=0.25$ (s^{-1}), and $\eta=6.7$. The arrow indicates the spatial coordinate where a transition from an oscillatory to excitable regime occurs (the Hopf bifurcation).

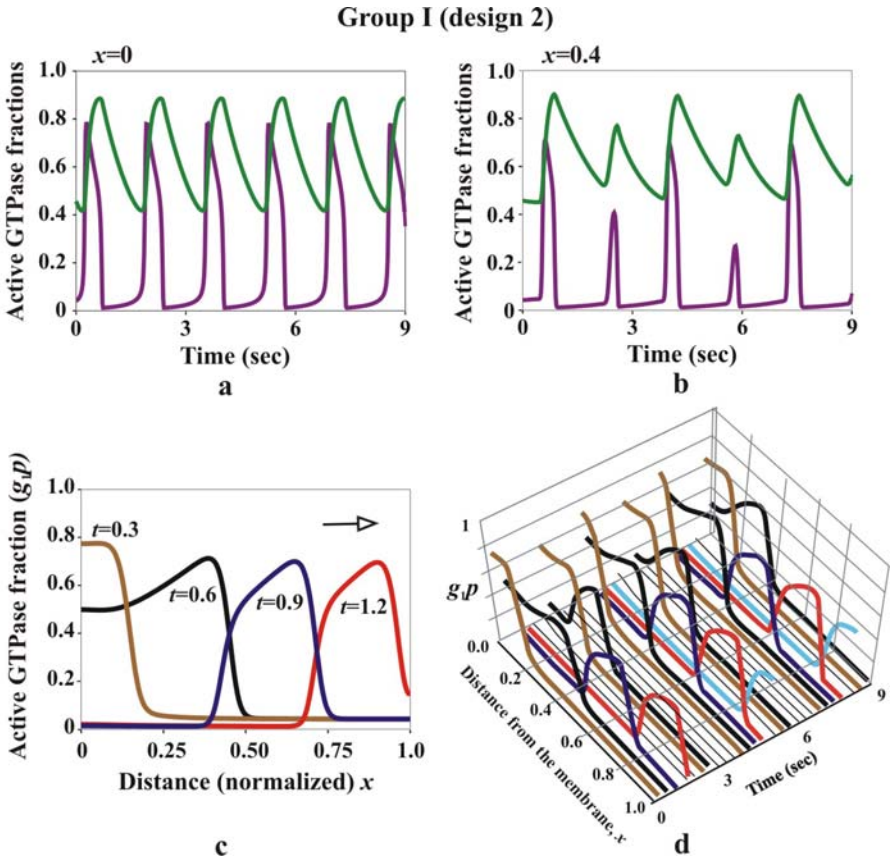

Fig. S6. Propagation or vanishing of periodic pulses in spatially heterogeneous media. The spatial gradient of GAP_2 constitutive activity is described by Eq. 10 (Methods) with slightly different kinetic parameters in comparison with Fig. 6, and Fig. S5: $r_4(0)=1$, $r_4(1)=0.5$, and $r_3= 0.4$ (s^{-1}). (**a**) Close to the membrane ($x \approx 0$), active GTPase fractions (g_1p, purple and g_2p, green) oscillate with a period of 1.5 s. A decrease in GAP_2 activity farther away from the membrane brings about the change in the cascade dynamics: oscillatory behavior is no longer observed, whereas excitable behavior emerges at $x \approx 0.2$ (the Hopf bifurcation). (**b**) Since this period of oscillations is smaller than the recovery time (known as the refractory period) of the emerging excitable media at the distance $x > 0.2$ from the membrane, not all oscillatory activity maxima lead to the formation of GTPase activity pulses with a large amplitude; some pulses become rather small and subsequently vanish during the propagation through the cell. (**c**) A pulse-like wave propagating through the cell is shown for a selected time window (0.3 - 1.2 s), using different colors for different time moments. (**c**) A 3-D presentation of propagating waves of periodic GTPase activity pulses driven by oscillating GTPase activities near the membrane. The remaining kinetic parameters and the initial GTPase activities, which correspond to a spatially homogeneous steady state, are given in Table S2.

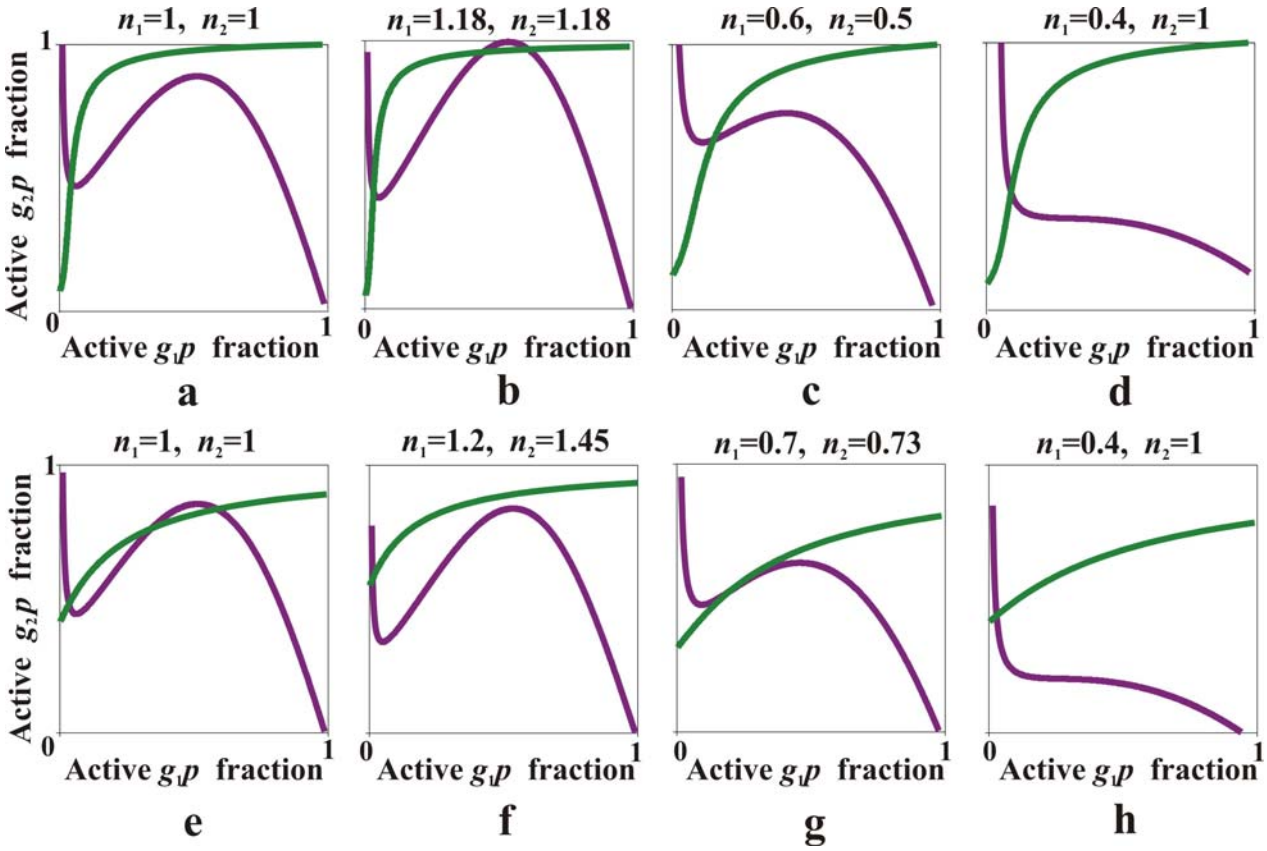

Fig. S7. Influence of the changes in the total GTPase abundances on the spatiotemporal cascade dynamics. The figure shows changes in the nullclines and the corresponding dynamic regimes following the alterations in the total abundance of the first and second GTPases (G_1^{tot} and G_2^{tot}), $G_{1new}^{tot} = n_1 \cdot G_1^{tot}$ and $G_{2new}^{tot} = n_2 \cdot G_2^{tot}$. According to Eqs. 1 -4 of the main text, this results in the following parameter changes: $m_1^{new} = m_1 / n_1$, $m_2^{new} = m_2 / n_1$, $m_3^{new} = m_3 / n_2$, $m_4^{new} = m_4 / n_2$, $m_{ij}^{new} = m_{ij} / n_i$. **a** -Excitable regime, the nullclines are calculated for parameter values given in Table S2. Following the changes in the total abundances as indicated by the coefficients n_1 and n_2, the system shifts to different dynamics regimes as follows, **b** - bistable, **c** - oscillatory, and **d** - monostable regimes. **e** -Bistable regime, the nullclines are calculated for parameter values given in Table S1. Following the changes in the total abundances as indicated by the coefficients n_1 and n_2, the system shifts to different dynamics regimes as follows, **f** -excitable, **g** - oscillatory, and **h** - monostable regimes.

Supplementary Documents.

Supplementary Document 1. Different design groups I - VIII are determined by the dimensionless multipliers α_{ij}.

Each cascade group I - VIII is characterized in by the values of the dimensional multipliers α_{ij}, as follows,

Groups I - IV are each hallmarked by an auto-activation loop, ($\alpha_{11} > 1$, $\alpha_{12} = 1$) or ($\alpha_{11} = 1$, $\alpha_{12} < 1$), and the remaining α_{ij} satisfy the following constraints,

Group I: ($\alpha_{21} < 1$, $\alpha_{22} = 1$) or ($\alpha_{21} = 1$, $\alpha_{22} > 1$); ($\alpha_{13} > 1$, $\alpha_{14} = 1$) or ($\alpha_{13} = 1$, $\alpha_{14} < 1$).

Group II: ($\alpha_{21} > 1$, $\alpha_{22} = 1$) or ($\alpha_{21} = 1$, $\alpha_{22} < 1$); ($\alpha_{13} < 1$, $\alpha_{14} = 1$) or ($\alpha_{13} = 1$, $\alpha_{14} > 1$).

Group III: ($\alpha_{21} > 1$, $\alpha_{22} = 1$) or ($\alpha_{21} = 1$, $\alpha_{22} < 1$); ($\alpha_{13} > 1$, $\alpha_{14} = 1$) or ($\alpha_{13} = 1$, $\alpha_{14} < 1$).

Group IV: ($\alpha_{21} < 1$, $\alpha_{22} = 1$) or ($\alpha_{21} = 1$, $\alpha_{22} > 1$); ($\alpha_{13} < 1$, $\alpha_{14} = 1$) or ($\alpha_{13} = 1$, $\alpha_{14} > 1$).

Groups V - VIII are each hallmarked by an auto-inhibition loop, ($\alpha_{11} < 1$, $\alpha_{12} = 1$) or ($\alpha_{11} = 1$, $\alpha_{12} > 1$), and the remaining α_{ij} satisfy the following constraints,

Group V: ($\alpha_{21} > 1$, $\alpha_{22} = 1$) or ($\alpha_{21} = 1$, $\alpha_{22} < 1$); ($\alpha_{13} > 1$, $\alpha_{14} = 1$) or ($\alpha_{13} = 1$, $\alpha_{14} < 1$).

Group VI: ($\alpha_{21} < 1$, $\alpha_{22} = 1$) or ($\alpha_{21} = 1$, $\alpha_{22} > 1$); ($\alpha_{13} < 1$, $\alpha_{14} = 1$) or ($\alpha_{13} = 1$, $\alpha_{14} > 1$).

Group VII: ($\alpha_{21} < 1$, $\alpha_{22} = 1$) or ($\alpha_{21} = 1$, $\alpha_{22} > 1$); ($\alpha_{13} > 1$, $\alpha_{14} = 1$) or ($\alpha_{13} = 1$, $\alpha_{14} < 1$).

Group VIII: ($\alpha_{21} > 1$, $\alpha_{22} = 1$) or ($\alpha_{21} = 1$, $\alpha_{22} < 1$); ($\alpha_{13} < 1$, $\alpha_{14} = 1$) or ($\alpha_{13} = 1$, $\alpha_{14} > 1$).

Supplementary Document 2. Relationships between kinetic parameters that enable identical steady states for molecular designs 1 - 8 comprising each topology group (I - VIII).

Using Table 1 (Methods), it is convenient to present the equations that determine nullclines for cascade designs 1 -8, as follows.

Definition of nullclines	Design 1	Design 2	Design 3	Design 4
$dg_1p/dt=0$ $dg_2p/dt=0$	$\alpha_{11}\alpha_{21}u_1-u_2=0$ $\alpha_{13}u_3-u_4=0$	$\alpha_{22}(\alpha_{11}\alpha_{22}^{-1}u_1-u_2)=0$ $\alpha_{13}u_3-u_4=0$	$\alpha_{12}\alpha_{22}(\alpha_{12}^{-1}\alpha_{22}^{-1}u_1-u_2)=0$ $\alpha_{13}u_3-u_4=0$	$\alpha_{12}(\alpha_{12}^{-1}\alpha_{21}u_1-u_2)=0$ $\alpha_{13}u_3-u_4=0$
	Design 5	Design 6	Design 7	Design 8
$dg_1p/dt=0$ $dg_2p/dt=0$	$\alpha_{11}\alpha_{21}u_1-u_2=0$ $\alpha_{14}(\alpha_{14}^{-1}u_3-u_4)=0$	$\alpha_{22}(\alpha_{11}\alpha_{22}^{-1}u_1-u_2)=0$ $\alpha_{14}(\alpha_{14}^{-1}u_3-u_4)=0$	$\alpha_{12}\alpha_{22}(\alpha_{12}^{-1}\alpha_{22}^{-1}u_1-u_2)=0$ $\alpha_{14}(\alpha_{14}^{-1}u_3-u_4)=0$	$\alpha_{12}(\alpha_{12}^{-1}\alpha_{21}u_1-u_2)=0$ $\alpha_{14}(\alpha_{14}^{-1}u_3-u_4)=0$

Comparing the nullcline equations of design 1 with such equations for designs 2 - 8 above, we can see that these nullclines become identical provided that the following relationships are satisfied:

Design 1 and Design 2:

$$\alpha_{11}^{(1)}\alpha_{21}^{(1)} = \alpha_{11}^{(2)}(\alpha_{22}^{(2)})^{-1} \Rightarrow \alpha_{11}^{(2)} = \alpha_{11}^{(1)},\ \alpha_{22}^{(2)} = 1/\alpha_{21}^{(1)} \Rightarrow \frac{1+a_{22}^{(2)}g_2 p/m_{22}^{(2)}}{1+g_2 p/m_{22}^{(2)}} = \frac{1+g_2 p/m_{21}^{(1)}}{1+a_{21}^{(1)}g_2 p/m_{21}^{(1)}} \Rightarrow$$

$$\Rightarrow (a_{22}^{(2)}a_{21}^{(1)}-1)g_2 p + (a_{22}^{(2)}m_{21}^{(1)} + a_{21}^{(1)}m_{22}^{(2)} - m_{21}^{(1)} - m_{22}^{(2)}) = 0 \Rightarrow a_{22}^{(2)}m_{21}^{(1)} + a_{21}^{(1)}m_{22}^{(2)} - m_{21}^{(1)} - m_{22}^{(2)} = 0 \Rightarrow$$

$$\Rightarrow m_{22}^{(2)}(a_{21}^{(1)}-1) = m_{21}^{(1)}(1-a_{22}^{(2)}) \Rightarrow \begin{cases} a_{22}^{(2)} = 1/a_{21}^{(1)} \\ m_{22}^{(2)} = m_{21}^{(1)}/a_{21}^{(1)} \end{cases}$$

Design 1 and Design 3:

$$\alpha_{11}^{(1)}\alpha_{21}^{(1)} = (\alpha_{12}^{(3)}\alpha_{22}^{(3)})^{-1} \Rightarrow \alpha_{12}^{(3)} = 1/\alpha_{11}^{(1)},\ \alpha_{22}^{(3)} = 1/\alpha_{21}^{(1)} \Rightarrow \begin{cases} a_{22}^{(3)} = 1/a_{21}^{(1)},\ m_{22}^{(3)} = m_{21}^{(1)}/a_{21}^{(1)} \\ a_{12}^{(3)} = 1/a_{11}^{(1)},\ m_{12}^{(3)} = m_{11}^{(1)}/a_{11}^{(1)} \end{cases}$$

Design 1 and Design 4:

$$\alpha_{11}^{(1)}\alpha_{21}^{(1)} = (\alpha_{12}^{(4)})^{-1}\alpha_{22}^{(4)} \Rightarrow \alpha_{22}^{(4)} = \alpha_{21}^{(1)},\ \alpha_{12}^{(4)} = 1/\alpha_{11}^{(1)} \Rightarrow a_{12}^{(4)} = 1/a_{11}^{(1)},\ m_{12}^{(4)} = m_{11}^{(1)}/a_{11}^{(1)}$$

Design 1 and Design 5:

$$\alpha_{11}^{(1)}\alpha_{21}^{(1)} = \alpha_{11}^{(5)}\alpha_{21}^{(5)} \Rightarrow \alpha_{11}^{(5)} = \alpha_{11}^{(1)},\ \alpha_{21}^{(5)} = \alpha_{21}^{(1)}$$

$$\alpha_{13}^{(1)} = (\alpha_{14}^{(5)})^{-1} \Rightarrow a_{14}^{(5)} = 1/a_{13}^{(1)},\ m_{14}^{(5)} = m_{13}^{(1)}/a_{13}^{(1)}$$

Design 1 and Design 6:

$$\begin{matrix} \alpha_{11}^{(1)}\alpha_{21}^{(1)} = \alpha_{11}^{(6)}(\alpha_{22}^{(6)})^{-1} \Rightarrow \alpha_{11}^{(6)} = \alpha_{11}^{(1)},\ \alpha_{22}^{(6)} = 1/\alpha_{21}^{(1)} \\ \alpha_{13}^{(1)} = (\alpha_{14}^{(6)})^{-1} \end{matrix} \Rightarrow \begin{cases} a_{22}^{(6)} = 1/a_{21}^{(1)},\ m_{22}^{(6)} = m_{21}^{(1)}/a_{21}^{(1)} \\ a_{14}^{(6)} = 1/a_{13}^{(1)},\ m_{14}^{(6)} = m_{13}^{(1)}/a_{13}^{(1)} \end{cases}$$

Design 1 and Design 7:

$$\begin{matrix} \alpha_{11}^{(1)}\alpha_{21}^{(1)} = (\alpha_{12}^{(7)}\alpha_{22}^{(7)})^{-1} \Rightarrow \alpha_{12}^{(7)} = 1/\alpha_{11}^{(1)},\ \alpha_{22}^{(7)} = 1/\alpha_{21}^{(1)} \\ \alpha_{13}^{(1)} = (\alpha_{14}^{(7)})^{-1} \end{matrix} \Rightarrow \begin{cases} a_{22}^{(7)} = 1/a_{21}^{(1)},\ m_{22}^{(7)} = m_{21}^{(1)}/a_{21}^{(1)} \\ a_{12}^{(7)} = 1/a_{11}^{(1)},\ m_{12}^{(7)} = m_{11}^{(1)}/a_{11}^{(1)} \\ a_{14}^{(7)} = 1/a_{13}^{(1)},\ m_{14}^{(7)} = m_{13}^{(1)}/a_{13}^{(1)} \end{cases}$$

Design 1 and Design 8:

$$\begin{matrix} \alpha_{11}^{(1)}\alpha_{21}^{(1)} = (\alpha_{12}^{(8)})^{-1}\alpha_{21}^{(8)} \Rightarrow \alpha_{12}^{(8)} = 1/\alpha_{11}^{(1)},\ \alpha_{21}^{(8)} = \alpha_{21}^{(1)} \\ \alpha_{13}^{(1)} = (\alpha_{14}^{(8)})^{-1} \end{matrix} \Rightarrow \begin{cases} a_{12}^{(8)} = 1/a_{11}^{(1)},\ m_{12}^{(8)} = m_{11}^{(1)}/a_{11}^{(1)} \\ a_{14}^{(8)} = 1/a_{13}^{(1)},\ m_{14}^{(8)} = m_{13}^{(1)}/a_{13}^{(1)} \end{cases}$$

The parameter relationships presented here in curly brackets are assembled in Table 1 (Methods).

Supplementary Document 3. Local stability and dynamic properties are identical for all 8 cascade circuitries within each of topology groups I - VIII.

We showed above that for the 8 different kinetic designs comprising each of groups I - VIII, the nullclines and steady states are identical if certain relationships between kinetic constants of regulatory interactions (feedback or feedforward loops) are fulfilled (Table 1, Methods and Supplementary material 2). Here we prove that the local stability and resulting dynamic properties of these designs are also the same. To simplify notations in the mathematical proofs, hereafter we designate the active GTPase fractions as follows,

$$y_1(t) = g_1 p(t),\ y_2(t) = g_2 p(t)\,.$$

It is convenient to introduce auxiliary parameters κ_1 and κ_2 as dimensionless multipliers, which modulate the rates (through modulation of constitutive GEF and GAP activities) at the first and second cascade layers, respectively. Thus, the parameter κ_1 is a dimensionless multiplier for the rates u_1 and u_2, and κ_2 is a multiplier of the rates u_3 and u_4. Using κ_1 and κ_2, the dynamics of cascade design 1 can be described as follows (see Eqs. 3, 4 in the main text and Table 1 in Methods),

$$\begin{aligned} \frac{dy_1}{dt} &= \kappa_1 \chi_1(y_1, y_2, p), \qquad \chi_1(y_1, y_2, p) = \alpha_{11}(y_1)\alpha_{21}(y_2)u_1(y_1) - u_2(y_1) \\ \frac{dy_2}{dt} &= \kappa_2 \chi_2(y_1, y_2, p), \qquad \chi_2(y_1, y_2, p) = \alpha_{13}(y_1)u_3(y_1, y_2) - u_4(y_2) \end{aligned} \qquad \text{(S1)},$$

where p is a vector of parameters, which include the kinetic constants and GEF and GAP concentrations (see Methods for the definitions of the functions α_{ij} and u_i).

If the relationships between kinetic parameters given in Table 1 (Methods) are fulfilled, the equations describing the dynamics of other designs 2 - 8, can be presented as,

$$\begin{aligned} \frac{dy_1}{dt} &= \varphi_1(y_1, y_2)\kappa_1 \chi_1(y_1, y_2, p) \\ \frac{dy_2}{dt} &= \varphi_2(y_1, y_2)\kappa_2 \chi_2(y_1, y_2, p) \end{aligned} \qquad \text{(S2)},$$

where the positive multipliers, $\varphi_i(y_1, y_2) > 0$, which determine a particular design are given in the table below,

	Designs							
	1	2	3	4	5	6	7	8
$\varphi_1(y_1, y_2) =$	1	$\alpha_{22}(y_2)$	$\alpha_{12}(y_1)\alpha_{22}(y_2)$	$\alpha_{12}(y_1)$	1	$\alpha_{22}(y_2)$	$\alpha_{12}(y_1)\alpha_{22}(y_2)$	$\alpha_2(y_1)$
$\varphi_2(y_1, y_2) =$	1	1	1	1	$\alpha_{14}(y_1)$	$\alpha_{14}(y_1)$	$\alpha_{14}(y_1)$	$\alpha_{14}(y_1)$

The steady states are determined as follows,

$$\frac{dy_1}{dt} = 0; \quad \frac{dy_2}{dt} = 0 \qquad \text{(S3)}.$$

One can readily see that the nullclines and steady states are identical for both systems 1 and 2 described by Eqs. S1 and S2, respectively. Let y_1^{ss}, y_2^{ss}, φ_1^{ss}, and φ_2^{ss} be the values of the variables y_1, y_2 and the functions φ_i at a particular steady state, where

$$\begin{aligned} &\chi_i(y_1^{ss}, y_2^{ss}, p) = 0 \\ &\varphi_i^{ss} = \varphi_i(y_1^{ss}, y_2^{ss}) > 0, \quad i = 1, 2 \end{aligned} \qquad \text{(S4)}.$$

We will next analyze the local stability (also termed exponential stability) of systems 1 and 2 near any steady state point. The Jacobian matrices ($\mathbf{J}_1$ and $\mathbf{J}_2$) for systems 1 and 2 at the steady state (y_1^{ss}, y_2^{ss}) are presented by Eqs. S5 and S6, respectively,

$$\mathbf{J}_1 = \begin{pmatrix} \kappa_1 \dfrac{\partial \chi_1}{\partial y_1} & \kappa_1 \dfrac{\partial \chi_1}{\partial y_2} \\ \kappa_2 \dfrac{\partial \chi_2}{\partial y_1} & \kappa_2 \dfrac{\partial \chi_2}{\partial y_2} \end{pmatrix}_{y_1^{ss}, y_2^{ss}} \tag{S5}.$$

$$\mathbf{J}_2 = \begin{pmatrix} \kappa_1 \left(\varphi_1 \dfrac{\partial \chi_1}{\partial y_1} + \chi_1 \dfrac{\partial \varphi_1}{\partial y_1} \right) & \kappa_1 \left(\varphi_1 \dfrac{\partial \chi_1}{\partial y_2} + \chi_1 \dfrac{\partial \varphi_1}{\partial y_2} \right) \\ \kappa_2 \left(\varphi_2 \dfrac{\partial \chi_2}{\partial y_1} + \chi_2 \dfrac{\partial \varphi_2}{\partial y_1} \right) & \kappa_2 \left(\varphi_2 \dfrac{\partial \chi_2}{\partial y_2} + \chi_2 \dfrac{\partial \varphi_2}{\partial y_2} \right) \end{pmatrix}_{y_1^{ss}, y_2^{ss}} = \begin{pmatrix} \varphi_1^{ss} \kappa_1 \dfrac{\partial \chi_1}{\partial y_1} & \varphi_1^{ss} \kappa_1 \dfrac{\partial \chi_1}{\partial y_2} \\ \varphi_2^{ss} \kappa_2 \dfrac{\partial \chi_2}{\partial y_1} & \varphi_2^{ss} \kappa_2 \dfrac{\partial \chi_2}{\partial y_2} \end{pmatrix}_{y_1^{ss}, y_2^{ss}} \tag{S6}.$$

We see that for system 2, the determinant of the Jacobian matrix $\mathbf{J}_2$ is multiplied by a positive factor that equals the product of φ_1^{ss} and φ_2^{ss}. Therefore, the condition det(**J**) = 0 will be true (or false) at the same parameter values for both systems 1 and 2. Consequently, if the saddle-node bifurcation occurs, it will take place for both systems simultaneously. However, Eq. S6 shows that the trace of the Jacobian is different for these two systems,

$$\mathrm{tr}(\mathbf{J}_1) = \kappa_1 \frac{\partial \chi_1}{\partial y_1} + \kappa_2 \frac{\partial \chi_2}{\partial y_2} \tag{S7}$$

and

$$\mathrm{tr}(\mathbf{J}_2) = \varphi_1^{ss} \kappa_1 \frac{\partial \chi_1}{\partial y_1} + \varphi_2^{ss} \kappa_2 \frac{\partial \chi_2}{\partial y_2} \tag{S8}.$$

Therefore, at first glance, the eigen values of the Jacobians $\mathbf{J}_1$ and $\mathbf{J}_2$ are not equal. Can we still say something about the local stability of a steady state of system 2, if we know the local stability of the same steady state of system 1?

Fortunately, the dimensionless multipliers, κ_1 and κ_2, can be modified without any change of the steady state values, y_1^{ss}, y_2^{ss}. If for system 2, we select the κ_1^* and κ_2^* values, as follows, $\varphi_1^{ss} \kappa_1^* = \kappa_1$, $\varphi_2^{ss} \kappa_2^* = \kappa_2$, then the Jacobians of both systems 1 and 2 become identical at the same steady state, y_1^{ss}, y_2^{ss},

$$\mathbf{J}_1(\kappa_1, \kappa_2) = \mathbf{J}_2(\kappa_1^*, \kappa_2^*).$$

This proves that both systems 1 and 2 (which are described by Eq. S1 and S2, respectively) can have the same Jacobian eigen values for the stationary solution, and thus possess similar local stability and dynamic properties (although at different parameter values, at the value κ_1 and κ_2 for system 1 and κ_1^* and κ_2^* for system S2).

Supplementary Document 4. Nullcline analysis.

First we show that for topology groups I - VIII, the g_2p-nullcline is a monotone function of g_1p for kinetic parameter values. Since for all 8 cascade designs within each topology group, the nullclines are identical when the proper relationships between the regulatory loop constants are fulfilled (see Table 1, Methods), we only consider nullclines for kinetic design 1.

As above, we simplify notations by designating $y_1(t) = g_1 p(t)$, $y_2 = g_2 p(t)$. For cascade design 1 in each topology group (I - VIII), the g_2p-nullcline ($dy_2/dt = 0$) is determined as follows (see Eqs. 3 and 4 and Table 1, Methods),

$$r_3 \cdot \frac{1 + a_{13} y_1 / m_{13}}{1 + y_1 / m_{13}} \cdot \frac{(1 - y_2)/m_3}{1 + (1 - y_2)/m_3} - r_4 \cdot \frac{y_2 / m_4}{1 + y_2 / m_4} = 0 \qquad \text{(S9)}.$$

Rearranging, we obtain,

$$(a_{13} - Y(y_2)) y_1 = m_{13}(Y(y_2) - 1) \qquad \text{(S10)}.$$

Here the function Y is introduced to simplify notations,

$$Y(y_2) = \frac{r_4 y_2 (m_3 + 1 - y_2)}{r_3 (m_4 + y_2)(1 - y_2)} \qquad \text{(S11)}.$$

We will show now that $a_{13} \neq Y$ for any y_2 value, $0 < y_2 < 1$. Assuming that $a_{13} - Y(y_2) = 0$ for some y_2, it follows that the right hand side of Eq. S10 should equal 0, that is, $Y(y_2) = 1$. Then from our initial assumption, a_{13} must be equal to 1. Recall that for design 1 in each topology group, $a_{13} \neq 1$, and so our assumption that $a_{13} - Y(y_2) = 0$ must be false, and this proves that $a_{13} \neq Y$.

Using Eq. S10, y_1 can be presented as the following function of y_2,

$$y_1(y_2) = m_{13} \frac{Y(y_2) - 1}{a_{13} - Y(y_2)} \qquad \text{(S12)}.$$

If the function $y_1(y_2)$ is not monotone, then the derivative dy_1 / dy_2 must equal zero at some y_2,

$$\frac{dy_1}{dy_2} = \frac{m_{13}(a_{13} - 1)}{(a_{13} - Y(y_2))^2} Y'(y_2) = 0 \qquad \text{(S13)}.$$

This implies that $dY / dy_2 = 0$ at some y_2. Differentiating Eq. S11 results in the following quadratic equation for the y_2 value(s), at which Eq. S13 holds,

$$(m_3 + m_4) y_2^2 - 2 m_4 y_2 + (m_3 + 1) m_4 = 0 \qquad \text{(S14)}.$$

Since the discriminant of this quadratic equation is negative,

$D = 4m_4^2 - 4(m_3 + 1)m_4(m_3 + m_4) = -4m_3(m_4^2 + (m_3 + 1)m_4) < 0$,

Eq. S13 does not have real value solutions. This proves that the g_2p-nullcline, $dy_2/dt = 0$, is a monotone function. From Eq. S13, we can see that the sign of the derivative, dy_2/dy_1 is determined by the

difference, $a_{13}-1$. If $a_{13}>1$, the g_2p-nullcline is a monotone increasing function of g_1p, and when $a_{13}<1$, the g_2p-nullcline is a monotone decreasing function. This proves that for cascade designs comprising groups I, III, V and VII, the g_2p-nullcline is a monotone increasing function, and this nullcline is a monotone decreasing function for cascades in groups II, IV, VI, VIII (see Fig. 3 and Fig. S2, S3 and S4).

Next we show that for topology groups V - VIII, the g_1p-nullcline is a monotone function of g_2p for any values of kinetic parameters. As above, it is sufficient to consider only kinetic design 1. The g_1p-nullcline for cascade design 1 can be determined from the following equation, $dy_1/dt = 0$,

$$r_1\frac{1+a_{11}\cdot y_1/m_{11}}{1+y_1/m_{11}}\frac{1+a_{21}\cdot y_2/m_{21}}{1+y_2/m_{21}}\frac{(1-y_1)/m_1}{1+(1-y_1)/m_1}-r_2\frac{y_1/m_2}{1+y_1/m_2}=0 \qquad \text{(S15)}.$$

Rearranging, we obtain,

$$(a_{21}-Z(y_1))y_2(y_1)=m_{21}(Z(y_1)-1) \qquad \text{(S16)}.$$

Here $$Z(y_1)=\frac{r_2y_1(m_1+1-y_1)(y_1+m_{11})}{r_1(m_2+y_1)(m_{11}+a_{11}y_1)(1-y_1)} \qquad \text{(S17)}.$$

Since for design 1 in each topology group, $a_{21}\neq 1$, it can be shown that $a_{21}\neq Z$ for any for any y_1 value, $0<y_1<1$. Similar to above, the assumption $a_{21}-Z=0$ for some y_2 would imply that a_{21} must be equal 1, which is untrue for design 1. From Eq. (S16), it follows that,

$$y_2(y_1)=m_{21}\frac{Z(y_1)-1}{a_{21}-Z(y_1)} \qquad \text{(S18)}.$$

If the function $y_2(y_1)$ is not monotone, then the derivative dy_2/dy_1 must equal zero at some y_1,

$$\frac{dy_2}{dy_1}=\frac{m_{21}(a_{21}-1)}{(a_{21}-Z(y_1))^2}Z'(y_1)=0 \qquad \text{(S19)}.$$

Differentiating the function Z, we obtain the following equation for the y_1 value that satisfies Eq. (S19),

$$c_4y_1^4+c_3y_1^3+c_2y_1^2+c_1y_1+c_0=0 \qquad \text{(S20)},$$

where the parameter values are given as follows,

$$\begin{aligned}
c_4&=m_{11}(1-a_{11})+a_{11}m_1+a_{11}m_2\\
c_3&=2(a_{11}m_{11}(m_1+1)+m_{11}m_2-m_{11}-a_{11}m_2)\\
c_2&=m_{11}{}^2m_2+m_{11}{}^2m_1+a_{11}m_{11}km_1+m_{11}(m_1+1)(1-a_{11})+a_{11}m_2(m_1+1)-m_{11}m_2(m_1+1)-3m_{11}m_2\\
c_1&=2(m_{11}m_2(m_1+1)-m_{11}{}^2m_2)\\
c_0&=m_{11}{}^2m_2(m_1+1)
\end{aligned} \qquad \text{(S21)}.$$

Taking Eq. S21 into consideration, it is convenient to regroup the different terms of Eq. S20, presenting this equation as the sum of the five following terms,

$$\mu_1+\mu_2+\mu_3+\mu_4+\mu_5=0 \qquad \text{(S22)},$$

where,

$$\mu_1 = a_{11}m_1y_1^4 + [m_{11}{}^2m_1 + a_{11}m_{11}m_2m_1]y_1^2$$
$$\mu_2 = m_{11}(1-a_{11})y_1^4 - 2m_{11}(1-a_{11}(m_1+1)y_1^3 + m_{11}(m_1+1)(1-a_{11})y_1^2 > m_{11}y_1^2(1-a_{11})[y_1^2 - 2y_1 + (m_1+1)]$$
$$\mu_3 = a_{11}m_2y_1^4 - 2a_{11}m_2y_1^3 + a_{11}m_2(m_1+1)y_1^2 = a_{11}m_2y_1^2(y_1^2 - 2y + (m_1+1)) = a_{11}m_2y_1^2[(y_1-1)^2 + m_1]$$
$$\mu_4 = m_{11}^2m_2y_1^2 - 2m_{11}^2m_2y_1 + m_{11}^2m_2(m_1+1) = m_{11}^2m_2(y_1^2 - 2y_1 + (m_1+1)) = m_{11}^2m_2[(y_1-1)^2 + m_1]$$
$$\mu_5 = 2m_{11}m_2y_1^3 - (3m_{11}m_2 + m_{11}m_2(m_1+1))y_1^2 + 2m_{11}m_2(m_1+1)y_1 = m_{11}m_2y_1[2y_1^2 - (4+m_1)y_1 + 2(m_1+1)] =$$
$$= 2(1-y_1)^2 + 2m_1(1-y_1) + m_1y_1$$

Since all kinetic constants are positive and $a_{11} < 1$ for each group V-VIII (hallmarked by an auto-inhibitory loop, Fig. 1b), one can readily see that each term (μ_1, μ_2, μ_3, μ_4, μ_5) is positive, and therefore the left-hand side of Eq. S20 is always positive. This proves that for cascade designs comprising groups V-VIII, Eq. S19 does not have solutions for any $0 < y_1 < 1$, and the g_1p-nullcline, $dy_1/dt = 0$, is monotone function. The sign of the derivative, dy_1/dy_2 is determined by the sign of the difference, $a_{21} - 1$ (see Eq. S13). If $a_{21} > 1$, the g_1p-nullcline is monotone increasing function, and when $a_{21} < 1$, the g_1p-nullcline is monotone decreasing function. This proves that for cascade designs in groups V and VIII, the g_1p-nullcline is a monotone increasing function, whereas for groups VI and VII the g_1p-nullcline is a monotone decreasing function (see Fig. 3 and Fig.S2).

Supplementary Document 5. Influence of small G-protein overexpression on the spatiotemporal cascade dynamics.

Many GTPases are overexpressed in cancer [1]. Although increases in the total GTPase abundances (G_1^{tot} and G_2^{tot}) can change the spatiotemporal dynamics, a particular G-protein cascade still belongs to the same topology group. In fact, different topology groups are determined by the dimensionless multipliers a_{ij} that do not depend on G_1^{tot} and G_2^{tot} (see Materials and Methods, Eqs 2 and 4, and Supplementary Document 1). Therefore, merely overexpression of small G-proteins, but not a mutation that can make it constantly active, does not change the types of possible dynamic behaviors in time and space. Moreover, under specific saturating conditions the basal GTPase fractions at steady state are relatively insensitive to GTPase overexpression [1]. Yet in the other cellular context, even relatively small variations in the total GTPase abundances can dramatically change the cascade dynamic behavior, as illustrated in Fig. S7.

References.

1. S. Legewie, C. Sers and H. Herzel, *FEBS Lett*, 2009, **583**, 93-96.

Table S1. Kinetic parameters of bistable regimes and active GTPase fractions (g_1p_{ss} and g_2p_{ss}) at two different steady states S_1 and S_2 for cascade design 1 in groups I – VI[*].

	Design 1											
	Group I		Group II		Group III		Group IV		Group V		Group VI	
r_1 (s^{-1})	5		10		1		1		1		1	
r_2 (s^{-1})	4		6.5		0.65		0.8		1.6		0.13	
r_3 (s^{-1})	0.13		0.4		0.5		0.1		1		1	
r_4 (s^{-1})	0.072		0.7		0.6		0.5		3		0.01	
m_1	0.7		25		25		0.7		1		0.4	
m_2	0.15		0.09		0.09		0.15		5		0.09	
m_3	0.6		5		5		0.8		2		0.1	
m_4	0.05		14		5.5		8		0.005		0.05	
a_{11}	200		200		200		200		0.01		0.6	
m_{11}	4		10		10		4		0.005		0.1	
a_{13}	100		0.005		40		0.05		100		0.004	
m_{13}	40		0.5		10		0.3		3		0.002	
a_{21}	0.02		80		80		0.02		100		0.01	
m_{21}	0.04		20		20		0.04		2		0.1	
	Steady states		Steady states		Steady states		Steady states		Steady states		Steady states	
	S_1	S_2	S_1	S_2	S_1	S_2	S_1	S_2	S_1	S_2	S_1	S_2
g_1p_{ss}	0.035	0.59	0.055	0.485	0.038	0.756	0.023	0.91	0.1	0.483	0.078	0.83
g_2p_{ss}	0.48	0.83	0.586	0.43	0.516	0.8	0.56	0.23	0.0045	0.49	0.94	0.68

[*]The input GEF_1 activity (parameter r_1) is varied to obtain the hysteretic plots shown in Fig. 3 (right panels) of the main text. In Figs. 5 and 6 of the main text the relationships between the kinetic parameters of designs 1 and 2 is given in Table I (Methods).

Table S2. Kinetic parameters of oscillatory and excitable regimes and active GTPase fractions (g_1p_{ss} and g_2p_{ss}) at steady states for cascade design 1 in groups I and II.

	Design 1					
	Group I			**Group II**		
	Oscillatory	**Excitable**		**Oscillatory**	**Excitable**	
$r_1(s^{-1})$	5	5		10	10	
$r_2(s^{-1})$	4	4		6.5	6.5	
$r_3(s^{-1})$	0.2	0.4*, 0.125*		1	0.55**, 1.7**	
$r_4(s^{-1})$	0.5	0.5		0.55	0.55	
m_1	0.7	0.7		25	25	
m_2	0.15	0.15		0.09	0.09	
m_3	0.6	0.6		5	5	
m_4	0.05	0.05		14	14	
a_{11}	200	200		200	200	
m_{11}	4	4		10	10	
a_{13}	100	100		0.005	0.005	
m_{13}	3	3		0.05	0.05	
a_{21}	0.02	0.02		80	80	
m_{21}	0.04	0.04		20	20	
	-----	Steady states		-----	Steady states	
		S_a	S_b		S_c	S_d
g_1p_{ss}	-----	0.044	0.59	-----	0.05	0.5
g_2p_{ss}		0.46	0.83		0.58	0.44

*Group I: r_3= 0.4 and steady state S_a correspond to Figs.4e, 5c and 6 of the main text and Fig.S4a; r_3= 0.125 and steady state S_b correspond to Figs. 4f and 5d of the main text and Fig.S4b.

**Group II: r_3= 0.55 and steady state S_c correspond to Fig. 4g of the main text and Fig.S4c; r_3= 1.7 and steady state S_d correspond to Fig. 4h of the main text and Fig.S4d.

For Fig. 4-6 of the main text the relationships between the kinetic parameters of designs 1, 2 and 5 are given in Table I (Methods).

Table S3. Kinetic parameters of bistable, oscillatory and excitable regimes and active GTPase fractions (g_1p_{ss} , g_2p_{ss} and g_3p_{ss}) at two different steady states S_1 and S_2 of a 3-tier cascade shown in Fig. 7 in the main text*

	Bistable		Oscillatory	Excitable
$r_1(s^{-1})$	1		1	8
$r_2(s^{-1})$	20		35	80
$r_3(s^{-1})$	5		50	50
$r_4(s^{-1})$	4		40	40
$r_5(s^{-1})$	0.12		0.12	0.12
$r_6(s^{-1})$	0.75		0.75	0.75
m_1	0.5		1.45	1.45
m_2	0.005		1.2	0.01
m_3	0.7		0.7	0.7
m_4	0.15		0.15	0.15
m_5	0.6		0.6	0.6
m_6	0.05		0.05	0.05
a_{13}	100		100	100
m_{13}	2		2	2
a_{21}	200		200	200
m_{21}	4		4	4
a_{25}	100		100	100
m_{25}	15		3	3
a_{34}	50		50	50
m_{34}	2		2	2
	Steady states		-	Steady state
	S_1	S_2		S
g_1p_{ss}	0.0025	0.456		0.003
g_2p_{ss}	0.19	0.91		0.11
g_3p_{ss}	0.014	0.09		0.04

*The steady-state values of active GTPase fractions (g_1p_{ss}, g_2p_{ss}, g_3p_{ss}) were used as the initial spatially homogeneous conditions in Fig. 7c (steady state S_1) and Fig. 7d (steady state S) of the main text. The initial perturbation in Fig. 7c was the following, $g_1p(x,0) = 0.8$ for $0 \le x \le 0.03$.